ECS Transactions, 64 (9) 159-166 (2014)
10.1149/06409.0159ecst ©The Electrochemical Society

Promoted Platinum Catalytic Activity and Thermal Stability with Nano-scale Cobalt Oxide Coating via Atomic Layer Deposition

Kun Cao[1], Bin Huang[1], Yihang Zhang[1], Xiao Liu[2], Bin Shan[1], and Rong Chen[2*]

[1]State Key Laboratory of Material Processing and Die & Mould Technology, School of Materials Science and Engineering,
[2]State Key Laboratory of Digital Manufacturing Equipment and Technology, School of Mechanical Science and Engineering,
Huazhong University of Science and Technology, 1037 Luoyu Road, Wuhan, Hubei PR China 430074
*Corresponding author: rongchen@mail.hust.edu.cn

Ultra-thin cobalt oxide has been deposited on the Pt nanoparticles to enhance the metal nanoparticles thermal stability. The thickness of protective Co_3O_4 coating layer can be accurately controlled around 1nm via atomic layer deposition. The Pt catalytic activity towards CO oxidation has been investigated in a micro flow reactor. In contrast to the aluminum oxide coating, the cobalt oxide coated Pt nanoparticles has demonstrated lower conversion temperature than bare Pt nanoparticles. Moreover the coated Pt nanoparticles show good sintering resistance up to 700℃ under atmosphere condition.

Introduction

Catalytic converters are required to control the emissions of CO, NO and hydrocarbons from automotive exhaust (1-3). Achieving lower temperature CO oxidation conversion is one of the important topics to solve the cold start problem. Platinum nanoparticles (NPs) are commonly used for three-way catalysts in CO oxidation due to their high activity and chemical stability (4-5). In this catalytic application, sintering of Pt NPs is a major problem in that the coalescence of NPs usually causes a decrease of catalyst activity (6-7). It is found that a thin coating layer on noble metal nanoparticles could suppress the sintering phenomenon (8). Among various coating methods, atomic layer deposition (ALD) shows its advantage in forming conformal coating layer with accurate film thickness control (9-11). Recent works encapsulate the palladium nanoparticles with porous Al_2O_3 through ALD effectively preventing NPs from sintering. The Al_2O_3 in the first few cycles was preferentially deposited onto corner-, step- and edge- sites of the noble metal catalysts leaving active facet exposed to gas reactants (12), thus the catalyst retains the activity and selectivity in the oxidation dehydrogenation of ethane (ODHE) reactions (13).

However as for CO oxidation, Ma et al. demonstrate that the gold NPs with ultra-thin inert SiO_2 coating layer have good sintering resistance up to 700°C, but with a loss of catalytic activity (14). Here we report the utilization of active oxide layer to encapsulate Pt NPs for CO oxidation. The active oxide coated catalysts have additional metal-oxide interfaces which may further improve the catalytic activity (15) besides good sintering resistance. We use Co_3O_4 as the active oxide encapsulation as it has been

proven to be active towards CO oxidation and also an excellent support material for Pt (16-18). The thickness of the cobalt oxide film is controlled by varying the number of ALD cycles. CO oxidation measurements were carried out in a micro flow reactor designed for planar model catalysts. Our results indicate that the optimal coating thickness is around 1nm, beyond which the promotional effect from the cobalt oxide and platinum interface begins decaying off. At the same time the coated catalysts have good thermal stability up to 700°C under atmospheric conditions.

Experimental

Planar metal/oxide catalyst synthesis

The growth of planar catalyst was performed in a commercial Picosun SUNALE^{TM} R200 atomic layer deposition system. Ultrahigh purity nitrogen (99.999%) continuously passed through the chamber and acted as carrier gas. During the whole ALD process the base pressure of the chamber was controlled below 4mbar. The substrates were p-type Si (100) wafers with ~2nm native oxide. All the Si wafers were sliced into $10\times20mm^2$ pieces to ensure the same surface area for the following catalysts test. Pt ALD process was performed with (methylcyclopentadienyl)-trimethylplatinum ($MeCpPtMe_3$) and O_2 as precursors carried out at 300°C. The Pt source was heated to 65°C to provide enough vapor pressure. The lines were kept at 80°C to avoid condensation. The Pt ALD sequence consisted of a 1.6s pulse of $MeCpPtMe_3$ and a 2s pulse of O_2. The 8s purge of N_2 was introduced between the precursor pulses to remove the residual precursor.

Cobalt oxide ALD was carried out at 150°C. At this deposition temperature the chemical composition of cobalt oxide is Co_3O_4 (to be submitted). The Cobaltocene ($Co(CP)_2$) and O_3 were used as precursors. O_3 was generated by feeding pure O_2 (99.999%) into an O_3 generator, which gave an O_3 concentration of about 11% in vol. The cobalt precursor was maintained at 100°C during deposition. The pulse time of $Co(CP)_2$ was 1.6s and for O_3 was 2s. The N_2 purge time between precursors pulse was 8s. The Al_2O_3 ALD was performed using alternative pulses of trimethyl aluminum (TMA) and deionized water at 180°C. The pulse time for both precursors was 0.1s. The N_2 purge time between precursor pulses was 8s.

Catalyst characterization

An atomic force microscope (Agilent 5500) was employed to analyze Pt catalysts morphology and particles density. The composition and binding energies were examined by X-ray photoelectron spectroscopy (XPS) on an ESCALAB 250 photoelectron spectroscope (Thermo Fisher Scientific Inc.) by using the Al Kα radiation. Transmission electron microscopy (TEM, Tecnai G2 20) was performed to characterize the ALD Pt nanoparticles morphology and crystal structure. The thickness of the ALD films is measured by spectroscopic ellipsometry (SE, J. A. woollam M2000). Cauchy mode was used to fit the film thickness of Co_3O_4 and Al_2O_3. The Pt film thickness was obtained from fitting through B-spline and Drude-Lorentz oscillator modeling. Grazing incidence X-ray diffraction (GIXRD, XRD-7000S) was utilized to characterize the ALD catalysts crystal structure.

Planar catalyst test

The planar catalysts toward CO oxidation measurements were performed with a micro flow reactor (Schematic shown in Figure 1) running at atmospheric pressure. The reactor has an interior diameter of 30mm and 0.5mm in height. The inlet and outlet channels have a small inner diameter of ~0.15mm.The reactant gas is 0.5% CO and 4.5% O_2 diluted in Ar and constantly passes through the reactor at 5sccm. The outlet gas composition was analyzed by feeding the gas through a capillary positioned 10mm above the sample. A mass spectrometer (MS, AMETEK Dycor System 200 LCD) was used to detect the CO, CO_2 and O_2 signals through the capillary. The MS signal was converted to a total conversion yield (%) using calibrated CO_2 cracking pattern to obtain the correct CO content at m/Z=28. The linear heating ramp is 3°C/min controlled using a programmable logic controller (PLC).

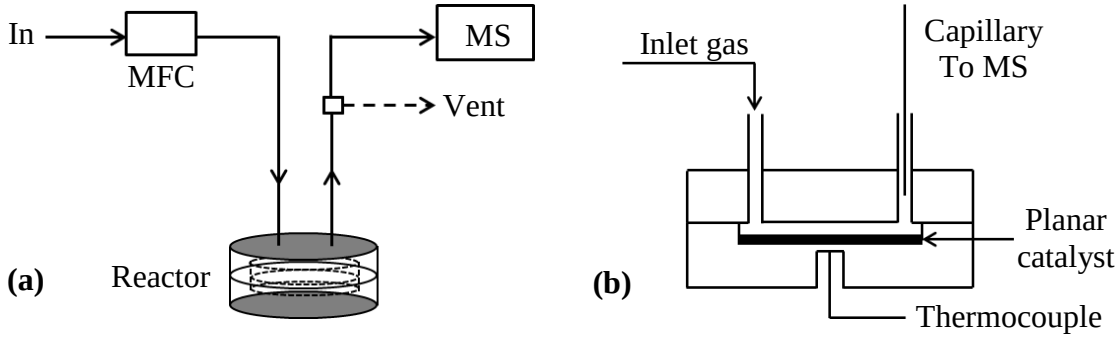

Figure 1. (a) Experiment setup of the planar catalytic test apparatus, (b) Schematic diagram of the micro flow reactor.

Results and Discussion

Pt nanoparticles catalyst synthesis

Due to the weak metal-organic chemisorption on oxide terminated substrates and the steric hindrance of the Pt precursor, the ALD of Pt exhibits a nucleation stage that the island-like NPs emerge at the beginning of the growth process. This kind of island-like growth mechanism demonstrates the Volmer-Weber growth mode, and it is advantageous to synthesize NPs for catalysis applications. At this period of stage, the average diameter of the Pt NPs increases almost linearly with the number of ALD cycles, corresponding to the ALD's conformal growth property. For TEM observation, the Pt NPs were grown on the carbon film grids pre-coated with ~3nm Al_2O_3 film via ALD. Figure 2 shows the TEM images Pt NPs of 50, 100, and 200 ALD cycles. As the ALD cycles increase, coalesce of Pt NPs takes a major role and finally forms a continuous film.

Crystal structures of Pt were identified from grazing incidence X-ray diffraction (GIXRD, incidence angle 2°). The GIXRD pattern demonstrates that the ALD Pt film is crystalline with face centered cubic (fcc) structure and (111) is the preferred orientation. TEM selected area electron diffraction (SAED) pattern of a 200 cycles Pt sample (not shown here) demonstrated that the Pt NPs show a metallic fcc structure. It is in consistent with the X-ray diffraction data.

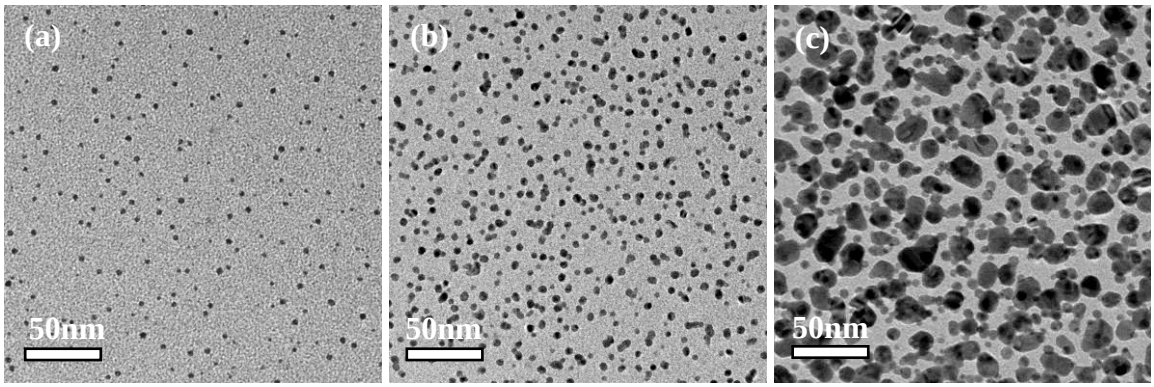

Figure 2. TEM images of (a) 50 cycles (b) 100 cycles and (c) 200 cycles of ALD Pt NPs on Al_2O_3 covered carbon film grids.

The growth rate of Al_2O_3, Pt and Co_3O_4 on Si wafer is shown in Figure 3 (a). For Al_2O_3 and Co_3O_4, liner growth is observed during the whole ALD process. Growth rate of thickness gain per cycle for Al_2O_3 is 0.96Å/cycle and 0.35Å/cycle for Co_3O_4. The Pt growth rate is lower at the first 100 cycles corresponding to the nucleation stage. Then it gradually increased to reach a steady-state growth rate of 0.62Å/cycle. X-ray photoelectron spectroscopy (XPS) was used to test the chemical state of the ALD Pt sample in Figure 3 (b). Pt $4f_{7/2}$ and Pt $4f_{5/2}$ peaks were clearly observed and located at 70.9eV and 74.2eV corresponding to the metallic Pt peaks.

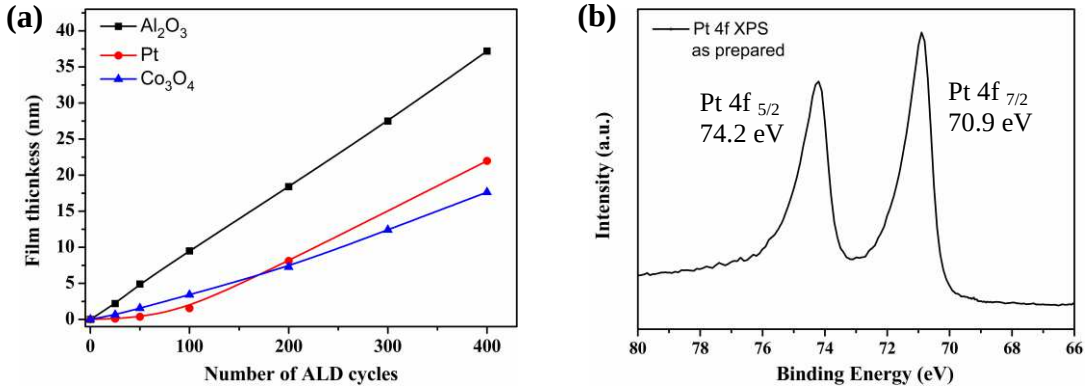

Figure 3. (a) Growth rate of Al_2O_3, Co_3O_4 and Pt on Si wafer, (b) XPS spectra of Pt 4f peaks.

CO oxidation on coated/uncoated Pt catalyst

Figure 4 (a) shows the CO to CO_2 conversion as a function of temperature obtained from 100 cycles Pt. From the calculation of SE measurement and Pt density, the total Pt loading of this sample is about ~6×10^{-3}mg. This total catalyst loading was orders of magnitude lower than that of Pt catalyst for powder test (for instance, 2% Pt loading on 50mg powder support). During the temperature increase, the $T_{50,\ up}$ (defined as the temperature corresponding to 50% of the maximum conversion during the temperature increase) was observed at 237°C. During cooling stage the $T_{50,\ down}$ changed to 225°C. This temperature hysteresis phenomenon is a normal behavior of Pt catalysts (19). During the temperature ramp up, after the reaction reaches complete conversion, the adsorbed CO is converted and the Pt active sites are covered with oxygen. In the temperature ramp down, the catalyst remains active even after the temperature is below the complete

conversion. The phenomenon may be attributed to the exothermic reaction of CO oxidation that keeps the local high temperature of the active sites.

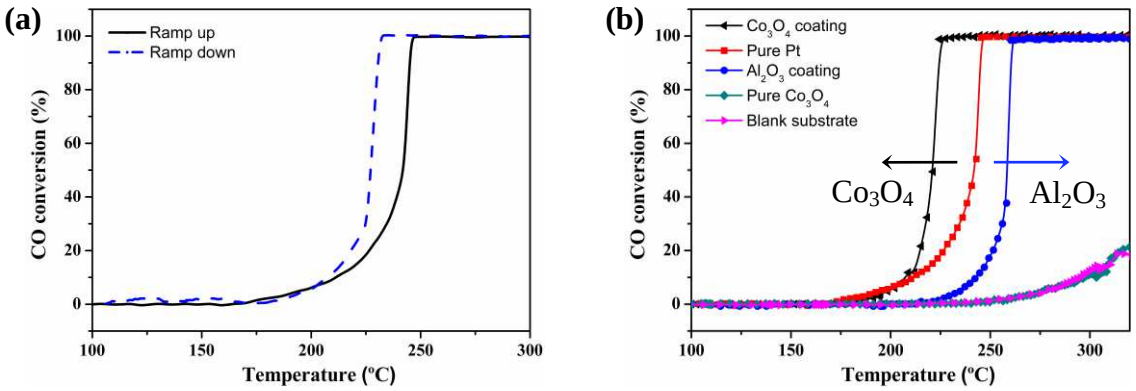

Figure 4. (a) CO oxidation on 100 cycles Pt catalyst, (b) light off curves on the planar catalysts

Then the Al_2O_3 and Co_3O_4 coated Pt catalysts activity was separately investigated (Figure 4 (b)). Al_2O_3 is usually used as protect layer to encapsulate the noble metal NPs to improve sintering resistance. For reactions such as methanol oxidation, a thin Al_2O_3 film coated Pd NPs showed improved catalyst activity and thermal stability (12). The deposition of Al_2O_3 in the first few cycles grows preferentially onto the low coordination sites and leaves active (111) facets exposed to methanol. For CO oxidation, an inert oxide coating layer may reduce the activity of the Pt NPs. In this study, the $T_{50, up}$ of Pt NPs with 9 cycles (~1nm) Al_2O_3 coating is 262°C, which is 25°C higher than the uncoated Pt catalysts. The results demonstrate that the inert oxide coating would reduce the catalytic activity for CO oxidation.

Then we investigated the influence of applying Co_3O_4 to coat the Pt NPs. Because the initial growth rate of Co_3O_4 is smaller than Al_2O_3, 25 cycles (~1nm) of Co_3O_4 was grown on the 100 cycles Pt NPs. From the light off curve of the Co_3O_4 coating Pt catalyst, the $T_{50, up}$ appeared at 219° C,which was 18° Clower than the uncoated Pt NPs and 43° Clower than Al_2O_3 coating Pt catalyst. Although Co_3O_4 is an active catalyst for CO oxidation, the 1nm Co_3O_4 alone did not exhibit catalytic activity as the light off curve overlap with the blanket substrate. Thus the significant enhancement of CO oxidation performance can be attributed to the cooperative effect of the metal-oxide interface. It is supposed that the redox behavior of the oxide provides the charge to alter the CO oxidation mechanism to charge transfer chemistry. A recent study (18) demonstrated that for the Co_3O_4 supported Pt catalyst, the Co^{2+} at the metal oxide interface is responsible for the improvement of the total catalyst activity.

Thermal stability of the Pt catalyst

To further investigate the thermal stability of the catalysts, a bare 100 cycles Pt catalyst sample, a 25 cycles Co_3O_4 coated Pt sample and a 9 cycles Al_2O_3 coated Pt sample were heated at 700° Cfor 2h under atmosphereic conditions. Figure 5 (a) and (b) show the AFM images of Co_3O_4 coated Pt sample and bare Pt sample before the heat treatment. Figure 5 (c) and (d) demonstrate the Co_3O_4 coated Pt sample and bare Pt sample after the heat treatment at 700° C for 2h under atmospheric conditions.

Figure 5 (d) shows significant sintering of the bare Pt NPs after heat treatment, many large particles (30-40nm) were observed during the aging treatment. Meanwhile the

density of Pt NPs has obviously decreased compared with the sample before heat treatment (Figure 5 (b)). For comparison, Pt NPs with Co_3O_4 coating layer did not sinter, minor morphology changes could be observed before and after the heat treatment (Figure (a) and (c)). The sintering resistance was also observed for the 9 cycles Al_2O_3 coated Pt NPs. The ALD Co_3O_4 coating on the Pt NPs as well as the support effectively stabilize the NPs by enhancing the NPs' bonding to the support (12). The NPs migration and coalescence are prevented and thus the thermal stability is increased. This method may also extend to other similar catalytic systems.

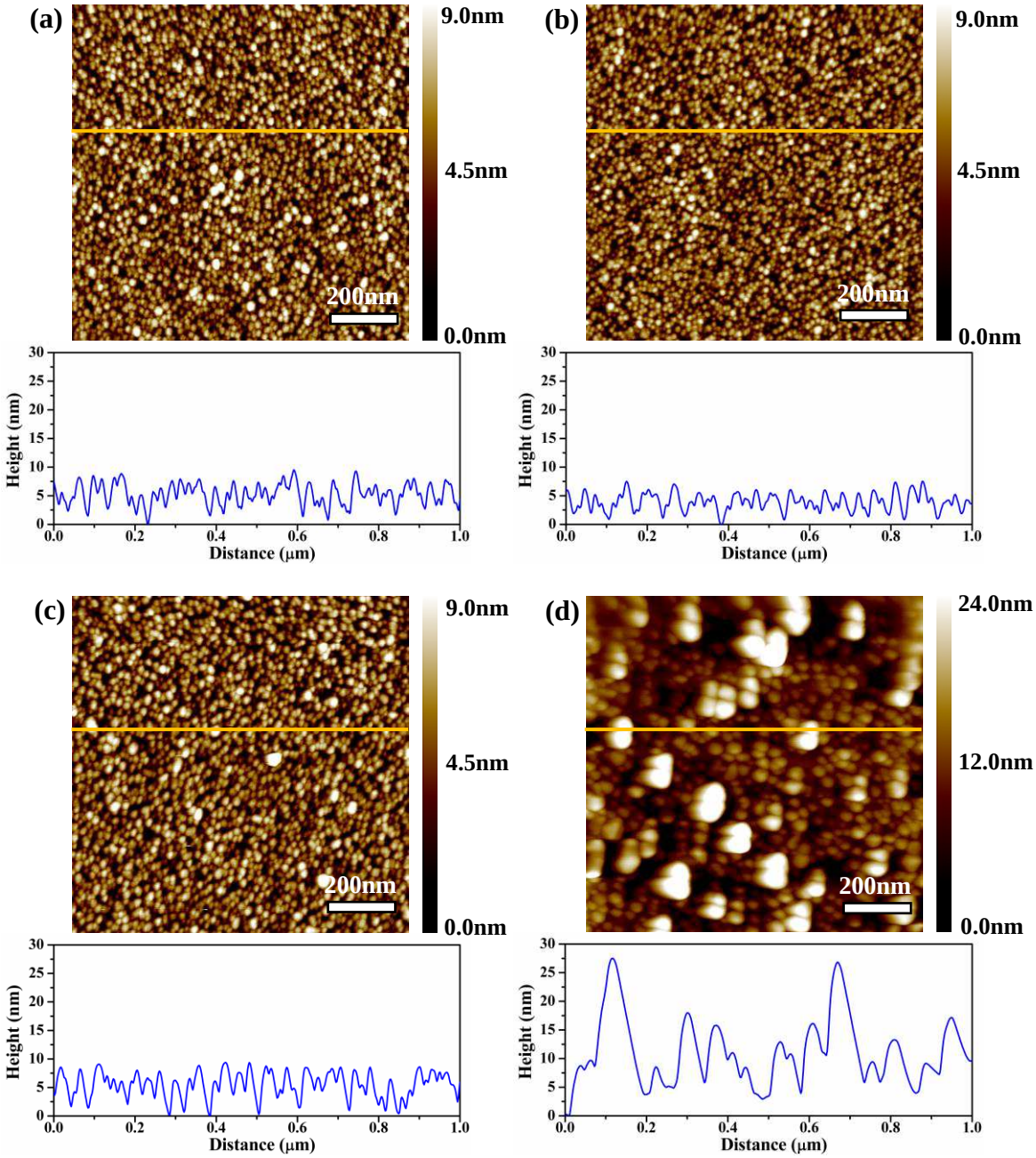

Figure 5. (a) 25 cycles Co_3O_4 coated Pt catalyst before heat treatment, (b) bare Pt catalyst before heat treatment, (c) 25 cycles Co_3O_4 coated Pt catalyst after heat treatment and (d) bare Pt catalyst after heat treatment. The cross-section height information is shown below the corresponding sample.

Conclusion

An ultra-thin cobalt oxide protective layer has been deposited on Pt nanoparticles via ALD to enhance catalytic performance and thermal stability. The CO oxidation reaction has been investigated in a micro flow reactor designed for the planar model catalysts. The results show that the Pt nanoparticles with ~1nm cobalt oxide coating layer show enhanced catalytic activity compared to pure Pt catalysts, while Pt NPs with the same thickness of Al_2O_3 protective layer show degraded activity. The promoted activity comes from the Pt-Co_3O_4 system rather than Co_3O_4 layer alone. The Co_3O_4 coated Pt NPs show good sintering resistance up to 700° Cunder atmospheric conditions. This work indicates that active oxide protective layers on Pt NPs could enhance both thermal stability and catalytic performance.

Acknowledgments

This work is supported by the National Basic Research Program of China (2013CB934800), National Natural Science Foundation of China (51101064), Fundamental Research Funds for the Central Universities, HUST (2014TS037). Rong Chen acknowledges the Thousand Young Talents Plan, the Recruitment Program of Global Experts and Program for Changjiang Scholars and Innovative Research Team in University. The authors also would like to acknowledge equipment supports from AMETEK lab and the technology support from the Analytic Testing Center of HUST.

References

1. B. R. Goldsmith, E. D. Sanderson, R. H. Quyang, W. X. Li, *J. Phys. Chem. C*, **118**, 9588, (2014)
2. Y. Gao, H. Oda, L. Jia, S. Amari, H. Kameyama, *Chemistry Letters*, **42**, 258, (2013)
3. M. P. Gonzalez-Marcos, B. Pereda, J. R. Gonzalez-Velasco, *Topics in Catalysis*, **56**, 352, (2013)
4. P. Bazin, O. Saur, O. Marie, V. Harle, G. Blanchard, *Applied Catalysis B:Environmental*, **119**, 207, (2012)
5. Z. Hu, F. M. Allen, C. Z. Wan, C. E. Lyman, *Journal of Catalysis*, **174**, 13, (1998)
6. J. Yang, V. Tschamber, P. Gilot, *Applied Catalysis B:Environmental*, **83**, 229, (2008)
7. F. Cabello Galisteo, C. Larese, R. Mariscal, *Topcis in Catalysis*, **30**, 451 (2004)
8. M. Seipenbusch, A. Binder, *J. Phys. Chem. C.*, **113**, 20606 (2009)
9. S.M. George, *Chem. Rev.*, **110**, 111 (2010)
10. M. Ritala, K. Kukli, J. Keinonen, *Science*, **288**, 319 (2000)
11. Riikka L. Puurunen, *J. Appl. Phys.*, **97**, 121301 (2005)
12. H. Feng, J. Lu, J. W. Elam, P. C. Stair, *Catal Lett.*, **141**, 512 (2011)
13. J. Lu, J. W. Elam, P. C. Stair, *Science.*, **8**, 2405 (2012)
14. Z. Ma, S. Brown, J. Y. Howe, S. Dai, *J. Phys. Chem. C.*, **112**, 9448 (2008)

15. J. A. Enterkin, W. Setthapum, J. W. Elam, C. L. Marshall, *ACS Catal.*, **1**, 629 (2011)
16. P. Thormahlen, M. Skoglundh, E. Fridell, B. Andersson, *Journal of Catalysis.*, **188**, 300 (1999)
17. Y. J. Mergler, A. van Aalst, B. E. Nieuwenhuys, *Applied Catalysis B: Environmental.*, **10**, 245 (1996)
18. A. Kwangjin, A. Selim, G. A. Somorjai, *J. Am. Chem. Soc.*, **135**, 16689 (2013)
19. C. Werdinius, L. Österlund, B. Kasemo, *Langmuir.*, **19**, 458 (2003)